

Published in Acta Phys. Pol. B 52, 1357 (2021)

Calculations of the alpha decay half-lives of some Polonium isotopes using the double folding model

W. A. YAHYA [†], K. J. OYEWUMI^{*}

[†]Department of Physics and Materials Science, Kwara State University, Malete, Kwara State, Nigeria

^{*}Department of Physics, University of Ilorin, Nigeria

The calculations of the alpha decay half-lives of some Polonium isotopes in the mass range 186 – 218 have been carried out using the Wentzel-Kramers-Brillouin (WKB) semiclassical approximation. The alpha-nucleus effective potential used contains the Coulomb potential, centrifugal potential, and the nuclear potential. The nuclear potential is obtained via the double folding model, with the microscopic NN effective interactions derived from relativistic mean field theory Lagrangian (termed R3Y). Different parametrizations of the R3Y interactions have been employed in the computation of the nuclear potentials. The results obtained using the R3Y NN interactions are compared with the ones obtained using the famous Michigan-3-Yukawa (M3Y) interactions. The use of density-dependent NN interaction is also considered. When compared to available experimental data, there are improvements in the results when density-dependent interaction potentials are used compared to when density-independent interactions are employed.

PACS numbers: 27.90.+b; 23.60.+e ; 21.10.Tg ; 23.70.+j

1. Introduction

Alpha decay is an important decay mode that can give information about the structure of nuclei [1, 2]. α -decay of nuclei have been investigated using various theoretical approaches such as the generalised liquid

[†] email: wasiu.yahya@gmail.com, wasiu.yahaya@kwasu.edu.ng

drop model [3–5], the effective liquid drop model [6], the modified generalized liquid drop model [7–9], the fission-like model [10], the preformed cluster model [11, 12], and cluster formation model [13–16]. These models use various interaction potentials ranging from the phenomenological potential such as the proximity potentials [17], the Woods-Saxon, squared Woods-Saxon, and Cosh potentials to microscopic interactions such as the double folding model. The Geiger-Nuttall law was the first decay law to describe α -decay half-life, and Gamow in 1928 gave a theoretical explanation of the Geiger-Nuttall law. Gamow explained that the α -decay was due to the quantum mechanical tunneling of a charged α particle through the nuclear Coulomb barrier [18]. Various empirical formulas have been introduced to compute the α -decay half-lives of many isotopes since the introduction of the Geiger-Nuttall law. Some of these formulas are the Royer formula [19–21], the Viola-Seaborg formula [22], the universal decay law developed by Qi et al. [23, 24], the Akrawy formula [25], the Ren formula, [26, 27], the scaling law of Horoi [28], scaling law of Brown, the AKRE formula developed by Akrawy and Poenaru [29], etc.

From a theoretical point of view, α -decay half-lives can be studied using the semiclassical WKB framework. In this formalism, the effective interaction between the alpha-daughter system plays an important role in the calculations. The effective interaction consists of the nuclear potential, the Coulomb potential and the centrifugal potential. There have been various phenomenological [30, 31] and microscopic nuclear potentials [32–36] introduced to study the α -decay of various nuclei. In the microscopic approach, the nuclear potential is determined using the double folding model, where the nuclear densities are folded with the effective M3Y nucleon-nucleon interaction. The use of density-dependent double folding model have also been introduced [36–38] to study the α -decay half-lives of many nuclei. A microscopic NN interaction derived from relativistic mean field theory Lagrangian (termed R3Y) was introduced in Ref. [12] where the authors used the derived NN interaction to compute the optical potential in the double folding model and studied cluster decays of some nuclei.

In this study, the α -decay half-lives of some Polonium isotopes have been calculated using both density-independent and density-dependent double folding model. The nuclear potential are calculated using the effective nucleon-nucleon interactions determined from relativistic mean field theory (termed R3Y). The results of the calculations using the M3Y-Paris and M3Y-Reid effective nucleon-nucleon interactions have also been included for comparison. The article is organised as follows: the theoretical models employed to compute the α -decay half-lives of the Polonium isotopes are

described in Section 2. The results of the calculations are presented and discussed in Section 3 while the conclusion is given in Section 4.

2. Theoretical Formalism

The effective alpha-nucleus potential $V(R)$ is given by

$$V_{eff}(R) = \lambda V_N(R) + V_C(R) + V_\ell, \quad (1)$$

where λ is the quantization factor, R is the relative distance between the alpha particle and daughter nucleus. The centrifugal term $V_\ell = \frac{\hbar^2 \ell(\ell+1)}{2\mu R^2}$, ℓ is the orbital angular momentum, $\mu = mA_1A_2/(A_1 + A_2)$ is the reduced mass of the α particle and the daughter nucleus, and the nucleon mass $m = 931.494$ MeV. By using Langer modification we have $\ell(\ell + 1) \rightarrow (\ell + \frac{1}{2})^2$. The values of ℓ are calculated by using the spin-parity selection rule [39]:

$$|J_d - J_p| \leq \ell \leq J_d + J_p, \quad (2)$$

$$\pi_p = (-1)^\ell \pi_d. \quad (3)$$

The Coulomb potential $V_C(R)$ is given in the form [36]

$$V_C(R) = Z_1 Z_2 e^2 \begin{cases} \frac{1}{R} & \text{for } R > R_C \\ \frac{1}{2R_C} \left[3 - \left(\frac{R}{R_C} \right)^2 \right] & \text{for } R \leq R_C \end{cases} \quad (4)$$

where Z_1 and Z_2 are the charge number of the alpha particle and daughter nucleus, respectively, and $R_C = 1.2 (A_1^{1/3} + A_2^{1/3})$.

The nuclear interaction potential $V_N(R)$ between the alpha and daughter nuclei in the double folding model is written as:

$$V_N(R) = \int \int \rho_1(\mathbf{r}_1) F(\rho_1, \rho_2) \rho_2(\mathbf{r}_2) v(E_\alpha, s) d\mathbf{r}_1 d\mathbf{r}_2, \quad (5)$$

where $s = |R + \mathbf{r}_2 - \mathbf{r}_1|$ is the relative distance between interacting nucleon pair, $\rho_1(\mathbf{r}_1)$ and $\rho_2(\mathbf{r}_2)$ are the ground state matter density distributions of the alpha and daughter nuclei, respectively, and the kinetic energy of the α particle is denoted as E_α . The density distribution of the alpha particle is taken to be the usual Gaussian form:

$$\rho_1(r_1) = 0.4299 e^{-0.7024 r_1^2}, \quad (6)$$

and the density distribution of the daughter nucleus is taken to be the Fermi form [37, 40]:

$$\rho_2(r_2) = \frac{\rho_0}{1 + \exp\left(\frac{r_2 - R}{a}\right)}, \quad (7)$$

where the diffuseness parameter $a = 0.54$ fm, $R_{1(2)} = 1.07A_{1(2)}^{1/3}$ (fm), A_1 is the mass number of the alpha particle and A_2 is the mass number of the daughter nucleus [37, 41]. The value of ρ_0 is obtained by integrating the matter density distribution equivalent to the mass number of the daughter nucleus.

In equation (5), the density-dependence factor $F(\rho, E_\alpha)$ is given as [42, 43]:

$$F(\rho_1, \rho_2) = C \left[1 + \alpha e^{-\beta(\rho_1 + \rho_2)} - \gamma(\rho_1 + \rho_2) \right]. \quad (8)$$

The parameters of the interaction viz. C , α , β , γ were determined through reproducing the saturation properties of normal nuclear matter within Hartree-Fock calculations [44]. The density-dependent NN interactions used in this paper is the DDM3Y1 parametrizations. The parameters C , α , β , γ corresponding to the DDM3Y1 parametrizations are given in Table 1.

Table 1: The parameters of the various density-dependent NN interactions used in this work [43–45].

Interaction	Label	C	α	β	γ
D-independent	DD0	1	0	0	0
DDM3Y1 (Reid)	DD1	0.2843	3.6391	2.9605	0.0000
DDM3Y1 (Paris)	DD1	0.2963	3.7231	3.7384	0.0000

The popular choices for nucleon-nucleon interactions in the double folding model have often been the M3Y interactions. The M3Y interactions were constructed to reproduce the G-matrix elements of both the Paris (M3Y-Paris) and Reid (M3Y-Reid) NN interactions in an oscillator basis [45]. They are given by:

$$v^{M3Y-Paris}(s, E_\alpha) = 11062 \frac{e^{-4s}}{4s} - 2537.5 \frac{e^{-2.5s}}{2.5s} + J_{00}^P(E_\alpha) \delta(\mathbf{s}) \quad (9)$$

and

$$v^{M3Y-Reid}(s, E_\alpha) = 7999 \frac{e^{-4s}}{4s} - 2134 \frac{e^{-2.5s}}{2.5s} + J_{00}^R(E_\alpha) \delta(\mathbf{s}) \quad (10)$$

respectively. In this study, the effective nucleon-nucleon interactions derived from relativistic mean field (RMF) theory Lagrangian, with different parametrizations are also employed. Following Ref. [12], the effective nucleon-nucleon interaction, derived from relativistic mean field Lagrangian is given by the sum of the scalar (σ) and vector (ω, ρ) parts of the meson fields. That is,

$$\begin{aligned} v_{eff}(s) &= V_\omega + V_\sigma + V_\rho \\ &= \frac{g_\omega^2}{4\pi} \frac{e^{-m_\omega s}}{s} - \frac{g_\sigma^2}{4\pi} \frac{e^{-m_\sigma s}}{s} + \frac{g_\rho^2}{4\pi} \frac{e^{-m_\rho s}}{s} + J_{00}(E) \delta(s), \end{aligned} \quad (11)$$

where g_i and m_i ($i = \omega, \sigma, \rho$) are the coupling constants and meson masses, respectively, and the last term is the exchange contribution. Different parameters of the RMF effective NN interaction have been employed in this work viz. R3Y-L1, R3Y-W, R3Y-Z, and R3Y-HS parametrizations. They are given, respectively, as [12]:

$$v^{R3Y-L1}(s, E_\alpha) = 9967.88 \frac{e^{-3.968s}}{4s} - 6660.95 \frac{e^{-2.787s}}{4s} + J_{00}^R(E_\alpha) \delta(\mathbf{s}), \quad (12)$$

$$v^{R3Y-W}(s, E_\alpha) = 8550.74 \frac{e^{-3.968s}}{4s} - 5750.24 \frac{e^{-2.787s}}{4s} + J_{00}^R(E_\alpha) \delta(\mathbf{s}), \quad (13)$$

$$v^{R3Y-Z}(s, E_\alpha) = 12008.98 \frac{e^{-3.9528s}}{4s} - 7861.80 \frac{e^{-2.7939s}}{4s} + J_{00}^R(E_\alpha) \delta(\mathbf{s}), \quad (14)$$

$$\begin{aligned} v^{R3Y-HS}(s, E_\alpha) &= 11956.94 \frac{e^{-3.968s}}{4s} - 6882.64 \frac{e^{-2.6352s}}{4s} \\ &+ 4099.06 \frac{e^{-3.902s}}{4s} + J_{00}^P(E_\alpha) \delta(\mathbf{s}). \end{aligned} \quad (15)$$

A complete description of the R3Y interactions is provided in Ref. [12]. The zero-range exchange terms are given by

$$J_{00}^R(E_\alpha) = -276(1 - 0.005E_\alpha/A_\alpha) \text{ MeV fm}^3 \quad (16)$$

and

$$J_{00}^P(E_\alpha) = -590(1 - 0.002E_\alpha/A_\alpha) \text{ MeV fm}^3. \quad (17)$$

Here $E_\alpha = Q_\alpha A_1/A$, Q_α denotes the energy released in the alpha decay process, and A is the mass number of the parent nucleus. The quantization factor λ in equation (1) is determined though the Bohr-Sommerfeld

quantization and Wildermuth rule [40, 41, 46]

$$\int_{r_1}^{r_2} \sqrt{\frac{2\mu}{\hbar} [Q_\alpha - V_{eff}(R)]} dR = (G - \ell + 1) \frac{\pi}{2}, \quad (18)$$

where the global quantum number, G , is given for α -decay process as

$$G_\alpha = \begin{cases} 18 & N \leq 82 \\ 20 & 82 < N \leq 126 \\ 22 & N > 126 \end{cases} . \quad (19)$$

The following formula is then used to calculate the α -decay half-life [41]:

$$T_{1/2} = \frac{\ln 2}{\nu P_\alpha P}, \quad (20)$$

where the assault frequency ν is determined using the WKB approximation [39]

$$\nu = \frac{\hbar}{2\mu} \left[\int_{r_1}^{r_2} \frac{dR}{\sqrt{\frac{2\mu}{\hbar^2} |Q - V_{eff}(R)|}} \right]^{-1} \quad (21)$$

and the tunneling probability P is calculated via

$$P = (1 + e^q)^{-1}, \quad (22)$$

and

$$q = \frac{\sqrt{8\mu}}{\hbar} \int_{r_2}^{r_3} \sqrt{V_{eff}(R) - Q} dR, \quad (23)$$

$r_i (i = 1, 2, 3)$ are the three turning points, and the pre-formation probability P_α is computed here using the empirical formula [39]:

$$\log P_\alpha = a\sqrt{\mu Z_1 Z_2} + b, \quad (24)$$

where $a = -0.052$ and $b = 0.69$ for even-even nuclei. For odd-A nuclei, $b = 0.6$.

3. Results and Discussions

Here the results of the calculations using the theory described above are presented and discussed. In the calculations, both density-independent (DDO) and density-dependent interactions (DDM3Y) were used. The experimental input data have been extracted from the NUBASE2020 database

[47–49]. In the calculations of the double folding potentials, the R3Y interactions with the different parametrizations (R3Y-HS, R3Y-L1, R3Y-W, and R3Y-Z) have been used. The calculations using the M3Y interactions are included for comparison with the R3Y interactions. In Figure 1, the plots of the effective alpha-nucleus interactions (equation (1)) using density-independent (DD0) R3Y-W, R3Y-L1, R3Y-HS, R3Y-Z, M3Y-Paris, and M3Y-Reid interactions are shown. The quantization factor (λ) is not included in Figure 1a, whereas it is used in Figure 1b. When the quantization factor is not included, the R3Y-Z can be seen to give the strongest potential while the M3Y-Reid gives the weakest potential. However when the quantization factor is used, only a slight difference is observed in the strengths of the potentials for the different models. The quantization factor has the most effect on the R3Y-Z potential, by drastically reducing the strength of the potential. The black dots in Figures 1a and 1b indicate the Q_α values.

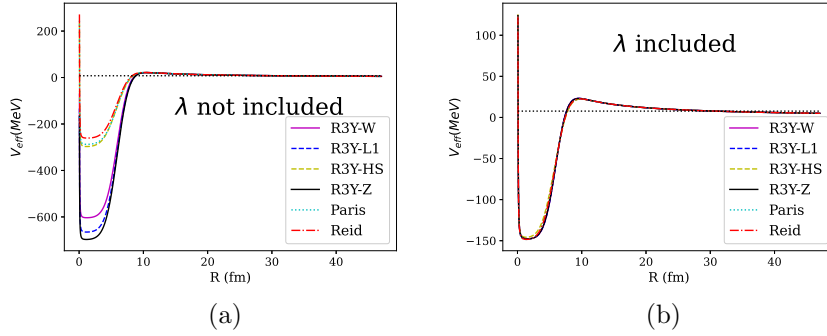


Fig. 1: Plot of the effective alpha-nucleus potential V_{eff} for ^{190}Po using density-independent (DD0) R3Y-W, R3Y-L1, R3Y-HS, R3Y-Z, M3Y-Paris, and M3Y-Reid interactions. (a) quantization factor not applied and (b) quantization factor included.

In order to give a quantitative comparison between the theoretically calculated results and the experimental data, the root mean square standard deviation (σ) has been computed for the different models. The following formula was used to compute the standard deviation: [17]:

$$\sigma = \sqrt{\frac{1}{N} \sum_{i=1}^N \left[\left(\log_{10} T_{1/2,i}^{\text{Theory}} - \log_{10} T_{1/2,i}^{\text{Expt}} \right)^2 \right]}. \quad (25)$$

Here $T_{1/2,i}^{\text{Expt}}$ are the experimental half-lives while $T_{1/2,i}^{\text{Theory}}$ are the theoretical

half-lives.

The calculated α -decay half-lives for the 33 Polonium (Po) isotopes using the double folding model with density-independent interactions (i.e. DD0) are shown in Table 2. Here the preformation factor P_α is taken to be one. The first three columns show, respectively, the mass number (A), experimental Q_α values, and the logarithm of the experimental α -decay half-lives. The fourth to ninth columns show the results using the M3Y-Paris, M3Y-Reid, R3Y-HS, R3Y-L1, R3Y-W, and R3Y-Z parameters, respectively. The last row of the Table shows the calculated standard deviation values (σ) for the various models. The σ for the M3Y-Paris, M3Y-Reid, R3Y-HS, R3Y-L1, R3Y-W, and R3Y-Z models are 0.8044, 0.8099, 0.7807, 0.5729, and 0.5595, respectively. The R3Y models have lower σ than the M3Y models, which suggests that the R3Y models give better descriptions of the α -decay half-lives of the Polonium isotopes than the M3Y models.

In Tables 3 and 4, the results of the calculated α -decay half-lives for the Polonium isotopes are shown using density-independent and density-dependent interactions, respectively. In both Tables, the pre-formation factor using equation (24) is included. The fourth to seventh columns show the results using the R3Y-HS, R3Y-L1, R3Y-W, and R3Y-Z models, respectively. The last column shows the calculated pre-formation factor ($\log P_\alpha$). A physical inspection of the Tables indicate that the R3Y-models give very good descriptions of the α -decay half-lives of the Polonium isotopes. Moreover, Table 5 shows the results of the standard deviation (σ) calculations using the data in Tables 3 and 4. When density-independent model is used, the four R3Y models viz. R3Y-HS, R3Y-L1, R3Y-W and R3Y-Z have the respective standard deviation values 0.4278, 0.4328, 0.4440, and 0.4159. This confirms that all the R3Y models give very good descriptions of the α -decay half-lives of the 33 polonium isotopes. The R3Y-Z gives the lowest value of σ while the R3Y-W gives the highest value. Furthermore, when the density-dependent interaction (DDM3Y) is used, the standard deviation values decrease for the four R3Y models. This shows the importance of using density-dependent interactions in the R3Y models.

The plots of the calculated α -decay half-lives $\log [T_{1/2}(s)]$ against the neutron number using the four R3Y-models with the experimental half-lives are shown in Figure 2. The density-independent model (DD0) is shown in Figure 2a while the density-dependent DDM3Y model is shown in Figure 2b. The maximum value of the α -decay half-lives is obtained at $N = 125$ which corresponds to the parent nucleus ^{209}Po . The minimum value of the α -decay half-lives is obtained at $N = 128$ which corresponds to the

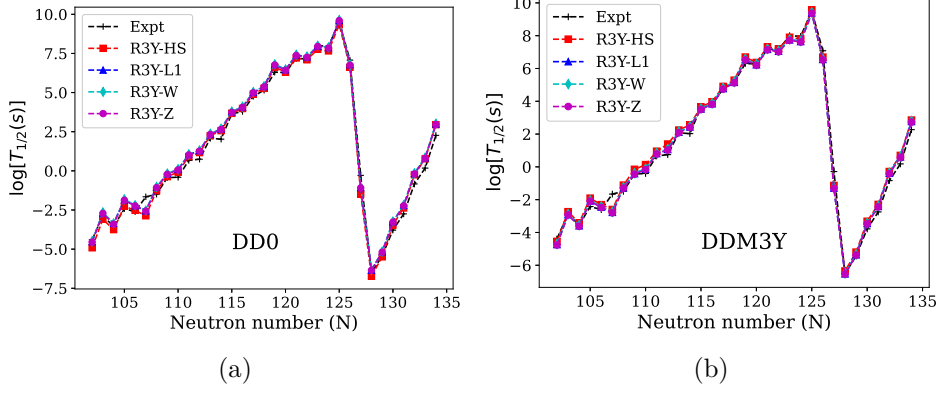


Fig. 2: Comparison of the calculated α -decay half-lives of the Po isotopes between the theoretical models and experiment. (a) using density-independent (DD0) interactions (b) using density-dependent DDM3Y interactions.

daughter nucleus ^{208}Pb with neutron number $N = 126$. The maximum and minimum values are associated with the role of shell closure effects relative to the magicity (or near magicity) of the neutron number. A high half-life indicates the magicity of the parent nucleus, while a low half-life indicates the magicity of the daughter nucleus. Here the daughter nucleus that corresponds to the lowest half-life (^{208}Pb) has a neutron magic number $N = 126$.

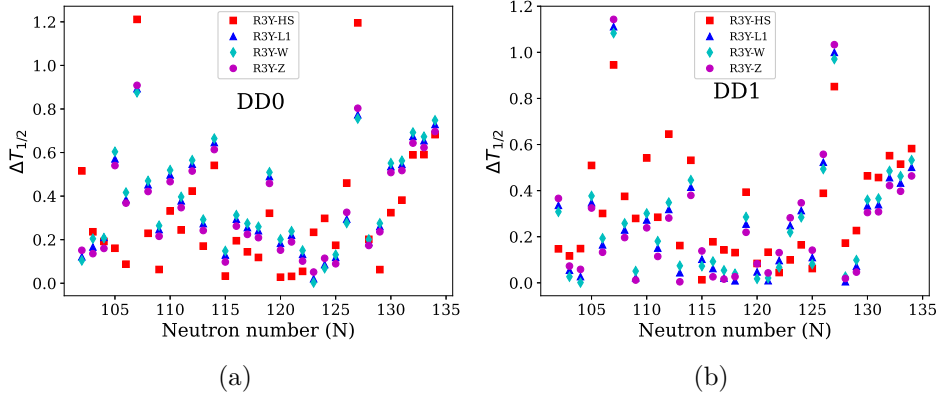


Fig. 3: Plot of the calculated $\Delta T_{1/2}$ against neutron number (N) for the Po (a) using density-independent (DD0) interactions (b) using density-dependent DDM3Y interactions.

Table 2: Calculated α -decay half-lives, $\log [T_{1/2}(s)]$, of Po isotopes ($Z = 84$) using density-independent (DD0) M3Y and R3Y interactions and setting $P_\alpha = 1$.

A	Q_α	$\log [T_{1/2}(s)]$						
		Expt.	M3Y-Paris	M3Y-Reid	R3Y-HS	R3Y-L1	R3Y-W	R3Y-Z
186	8.5012	-4.3980	-5.4067	-5.3986	-5.5411	-5.1470	-5.1298	-5.1767
187	7.9789	-2.8540	-3.6645	-3.6744	-3.8078	-3.4051	-3.3669	-3.4357
188	8.0823	-3.5610	-4.2642	-4.2736	-4.3805	-3.9779	-3.9813	-4.0288
189	7.6943	-2.4200	-2.8340	-2.8430	-2.9770	-2.5668	-2.5340	-2.5976
190	7.6933	-2.6090	-3.1242	-3.1327	-3.1493	-2.8523	-2.8201	-2.8689
191	7.8223	-1.6580	-3.5370	-3.5456	-3.5871	-3.2693	-3.2521	-3.2844
192	7.3196	-1.4920	-1.9469	-1.9498	-1.8905	-1.6678	-1.6500	-1.6987
193	7.0938	-0.4320	-1.1873	-1.1942	-1.0868	-0.9034	-0.8855	-0.9345
194	6.9871	-0.4070	-0.8235	-0.8301	-0.7033	-0.5378	-0.5157	-0.5689
195	6.7497	0.6670	0.0367	0.0306	0.1934	0.3272	0.3455	0.2959
196	6.6582	0.7450	0.3714	0.3654	0.5402	0.6635	0.6817	0.6319
197	6.4113	2.0800	1.3394	1.3337	1.5323	1.6357	1.6541	1.6038
198	6.3097	2.0260	1.7461	1.7403	1.9388	2.0435	2.0620	2.0113
199	6.0743	3.6400	2.7518	2.7463	2.9546	3.0513	3.0698	3.0192
200	5.9816	3.7900	3.1562	3.1504	3.3567	3.4558	3.4743	3.4237
201	5.7993	4.7600	3.9990	3.9934	4.1857	4.2972	4.3160	4.2657
202	5.7010	5.1500	4.4653	4.4593	4.6398	4.7626	4.7808	4.7307
203	5.4960	6.3000	5.7751	5.7683	5.9027	6.0713	6.0908	6.0396
204	5.4849	6.2800	5.5427	5.5365	5.6790	5.8348	5.8530	5.8032
205	5.3247	7.1800	6.3955	6.3892	6.4928	6.6820	6.7000	6.6509
206	5.3270	7.1500	6.3681	6.3615	6.4666	6.6538	6.6718	6.6228
207	5.2159	8.0000	6.9800	6.9725	7.0472	7.2603	7.2781	7.2297
208	5.2157	7.9610	6.9662	6.9592	7.0341	7.2459	7.2632	7.2174
209	4.9792	9.5070	8.6379	8.6304	8.6136	8.9069	8.9190	8.8773
210	5.4075	7.0780	5.8673	5.8609	5.9888	6.1545	6.1724	6.1233
211	7.5946	-0.2870	-2.0614	-2.0684	-2.2014	-1.7798	-1.7619	-1.8096
212	8.9542	-6.5240	-7.1707	-7.1783	-7.3548	-6.9657	-6.9520	-6.9799
213	8.5361	-5.4290	-6.1067	-6.1075	-6.2109	-5.8874	-5.8731	-5.9122
214	7.8335	-3.7840	-4.1262	-4.1323	-4.0893	-3.8779	-3.8620	-3.9052
215	7.5263	-2.7490	-3.1842	-3.1898	-3.0869	-2.9226	-2.9061	-2.9511
216	6.9063	-0.8390	-1.0826	-1.0937	-0.8790	-0.7942	-0.7763	-0.8251
217	6.6621	0.1800	-0.1825	-0.1871	0.0510	0.1151	0.1334	0.0834
218	6.1148	2.2690	2.0579	2.0532	2.3217	2.3686	2.3875	2.3357
σ			0.8044	0.8099	0.7807	0.5729	0.5595	0.5950

Table 3: Calculated α -decay half-lives, $\log [T_{1/2}(s)]$, of Po isotopes ($Z = 84$) using density-independent (DD0) interactions and including the preformation factor P_α

A	Q_α	$\log [T_{1/2}(s)]$					$\log P_\alpha$
		Expt.	R3Y-HS	R3Y-L1	R3Y-W	R3Y-Z	
186	8.5012	-4.3980	-4.9137	-4.5195	-4.5024	-4.5493	-0.6274
187	7.9789	-2.8540	-3.0902	-2.6876	-2.6494	-2.7182	-0.7175
188	8.0823	-3.5610	-3.7529	-3.3503	-3.3537	-3.4012	-0.6276
189	7.6943	-2.4200	-2.2593	-1.8492	-1.8163	-1.8799	-0.7177
190	7.6933	-2.6090	-2.5216	-2.2246	-2.1923	-2.2411	-0.6278
191	7.8223	-1.6580	-2.8693	-2.5515	-2.5343	-2.5666	-0.7178
192	7.3196	-1.4920	-1.2626	-1.0399	-1.0221	-1.0708	-0.6279
193	7.0938	-0.4320	-0.3689	-0.1855	-0.1675	-0.2165	-0.7180
194	6.9871	-0.4070	-0.0753	0.0903	0.1123	0.0592	-0.6280
195	6.7497	0.6670	0.9115	1.0453	1.0636	1.0140	-0.7181
196	6.6582	0.7450	1.1684	1.2916	1.3099	1.2601	-0.6282
197	6.4113	2.0800	2.2506	2.3539	2.3723	2.3220	-0.7183
198	6.3097	2.0260	2.5671	2.6719	2.6903	2.6396	-0.6283
199	6.0743	3.6400	3.6730	3.7697	3.7882	3.7376	-0.7184
200	5.9816	3.7900	3.9852	4.0843	4.1028	4.0522	-0.6285
201	5.7993	4.7600	4.9042	5.0157	5.0345	4.9842	-0.7185
202	5.7010	5.1500	5.2684	5.3913	5.4094	5.3593	-0.6286
203	5.4960	6.3000	6.6214	6.7900	6.8095	6.7583	-0.7187
204	5.4849	6.2800	6.3078	6.4635	6.4818	6.4320	-0.6287
205	5.3247	7.1800	7.2116	7.4008	7.4188	7.3697	-0.7188
206	5.3270	7.1500	7.0955	7.2827	7.3007	7.2517	-0.6289
207	5.2159	8.0000	7.7661	7.9793	7.9970	7.9486	-0.7189
208	5.2157	7.9610	7.6631	7.8749	7.8922	7.8464	-0.6290
209	4.9792	9.5070	9.3326	9.6260	9.6380	9.5963	-0.7190
210	5.4075	7.0780	6.6179	6.7836	6.8015	6.7524	-0.6291
211	7.5946	-0.2870	-1.4823	-1.0606	-1.0427	-1.0905	-0.7192
212	8.9542	-6.5240	-6.7256	-6.3365	-6.3228	-6.3506	-0.6292
213	8.5361	-5.4290	-5.4916	-5.1681	-5.1538	-5.1929	-0.7193
214	7.8335	-3.7840	-3.4600	-3.2485	-3.2327	-3.2758	-0.6293
215	7.5263	-2.7490	-2.3675	-2.2032	-2.1867	-2.2317	-0.7194
216	6.9063	-0.8390	-0.2495	-0.1647	-0.1468	-0.1957	-0.6295
217	6.6621	0.1800	0.7705	0.8346	0.8529	0.8029	-0.7195
218	6.1148	2.2690	2.9513	2.9981	3.0171	2.9652	-0.6296

Table 4: Calculated α -decay half-lives, $\log [T_{1/2}(s)]$, of Po isotopes ($Z = 84$) using density-dependent (DDM3Y) interactions and including the preformation factor P_α

A	Q_α	$\log [T_{1/2}(s)]$					$\log P_\alpha$
		Expt.	R3Y-HS	R3Y-L1	R3Y-W	R3Y-Z	
186	8.5012	-4.3980	-4.5453	-4.7343	-4.7061	-4.7643	-0.6274
187	7.9789	-2.8540	-2.7375	-2.9087	-2.8805	-2.9267	-0.7175
188	8.0823	-3.5610	-3.4126	-3.5880	-3.5600	-3.6193	-0.6276
189	7.6943	-2.4200	-1.9107	-2.0720	-2.0431	-2.0955	-0.7177
190	7.6933	-2.6090	-2.3080	-2.4443	-2.4158	-2.4764	-0.6278
191	7.8223	-1.6580	-2.6032	-2.7693	-2.7412	-2.8009	-0.7178
192	7.3196	-1.4920	-1.1169	-1.2627	-1.2339	-1.2957	-0.6279
193	7.0938	-0.4320	-0.1526	-0.4102	-0.3812	-0.4440	-0.7180
194	6.9871	-0.4070	0.1346	-0.1342	-0.1058	-0.1684	-0.6280
195	6.7497	0.6670	0.9515	0.8178	0.8476	0.7814	-0.7181
196	6.6582	0.7450	1.3903	1.0634	1.0933	1.0261	-0.6282
197	6.4113	2.0800	2.2417	2.1237	2.1540	2.0844	-0.7183
198	6.3097	2.0260	2.5576	2.4411	2.4714	2.4055	-0.6283
199	6.0743	3.6400	3.6532	3.5376	3.5676	3.5017	-0.7184
200	5.9816	3.7900	3.9680	3.8520	3.8825	3.8161	-0.6285
201	5.7993	4.7600	4.9028	4.7805	4.8143	4.7439	-0.7185
202	5.7010	5.1500	5.2811	5.1589	5.1894	5.1233	-0.6286
203	5.4960	6.3000	6.6933	6.5548	6.5854	6.5192	-0.7187
204	5.4849	6.2800	6.3641	6.2324	6.2625	6.1974	-0.6287
205	5.3247	7.1800	7.3128	7.1707	7.2009	7.1369	-0.7188
206	5.3270	7.1500	7.1946	7.0534	7.0829	7.0192	-0.6289
207	5.2159	8.0000	7.9006	7.7514	7.7806	7.7179	-0.7189
208	5.2157	7.9610	7.7963	7.6475	7.6766	7.6140	-0.6290
209	4.9792	9.5070	9.5689	9.3973	9.4263	9.3653	-0.7190
210	5.4075	7.0780	6.6895	6.5548	6.5843	6.5203	-0.6291
211	7.5946	-0.2870	-1.1383	-1.2869	-1.2578	-1.3202	-0.7192
212	8.9542	-6.5240	-6.3515	-6.5192	-6.4972	-6.5430	-0.6292
213	8.5361	-5.4290	-5.2023	-5.3571	-5.3304	-5.3826	-0.7193
214	7.8335	-3.7840	-3.3201	-3.4498	-3.4241	-3.4791	-0.6293
215	7.5263	-2.7490	-2.2922	-2.4099	-2.3831	-2.4409	-0.7194
216	6.9063	-0.8390	-0.2873	-0.3826	-0.3536	-0.4172	-0.6295
217	6.6621	0.1800	0.6948	0.6129	0.6427	0.5772	-0.7195
218	6.1148	2.2690	2.8513	2.7702	2.8012	2.7327	-0.6296

Table 5: The calculated root mean square standard deviations

	R3Y-HS	R3Y-L1	R3Y-W	R3Y-Z
DD0	0.4278	0.4328	0.4440	0.4159
DDM3Y	0.3970	0.3627	0.3651	0.3626

The difference between the experimental and theoretical α -decay half-lives has also been calculated using the following formula [17,27]:

$$\Delta T_{1/2} = \left| \log_{10} \left[T_{1/2}^{\text{theor}} \right] - \log_{10} \left[T_{1/2}^{\text{expt}} \right] \right|. \quad (26)$$

Figure 3 shows the plots of $\Delta T_{1/2}$ against neutron number for the different models. In Figure 3a, the computed $\Delta T_{1/2}$ using the density-independent models (DD0) are shown while Figure 3b shows the results using the density-dependent DDM3Y models. In the two plots (Figure 3a and Figure 3b), most of the points are below 0.6. This again confirms the accuracy of the use of the R3Y models to study the α -decay half-lives of the Polonium isotopes.

4. Conclusion

The calculations of the α -decay half-lives of some Polonium isotopes in the mass range 186–218 have been carried out theoretically using the WKB semiclassical approximations and with the use of the Bohr-Sommerfeld quantization factor. The α -nucleus potential is obtained using the double folding model, with the R3Y nucleon-nucleon effective interactions. The R3Y effective nucleon-nucleon interactions are derived from relativistic mean field theory Lagrangian. For comparison, the calculations using the M3Y interactions were also included. When compared with experimental data, the results obtained using the R3Y models are found to be better than the results obtained using the M3Y-Reid and M3Y-Paris NN interactions. When density-dependent DDM3Y interactions are used in the R3Y models, the results are found to be better than using density-independent interactions, with the R3Y-Z giving the lowest deviation from experimental data. In general, when compared to experimental data, the R3Y models give maximum standard deviation value $\sigma = 0.4440$ when density-independent interaction is used and maximum $\sigma = 0.3970$ when density-dependent interaction is employed. This shows the importance of using density-dependent interaction in the R3Y model. We conclude that the use of the R3Y effective NN interactions in the double folding model give very good descriptions of the alpha-decay half-lives of the Polonium isotopes.

REFERENCES

- [1] E. Shin, Y. Lim, C. H. Hyun, and Y. Oh. Nuclear isospin asymmetry in α decay of heavy nuclei. *Physical Review C*, 94(2):024320, 2016.

- [2] V. Zanganah, Dashty T. Akrawy, H. Hassanabadi, S.S. Hosseini, and Sha-gun Thakur. Calculation of α -decay and cluster half-lives for $^{197-226}\text{Fr}$ using temperature-dependent proximity potential model. *Nuclear Physics A*, 997:121714, 2020.
- [3] G. Royer and R. Moustabchir. Light nucleus emission within a generalized liquid-drop model and quasimolecular shapes. *Nuclear Physics A*, 683:182–206, 2001.
- [4] B. Xiaojun, H. Zhang, H. Zhang, G. Royer, and J. Li. Systematical calculation of α decay half-lives with a generalized liquid drop model. *Nuclear Physics A*, 921:85–95, 2014.
- [5] G. Royer and H. F. Zhang. Recent α decay half-lives and analytic expression predictions including superheavy nuclei. *Physical Review C*, 77:037602, 2008.
- [6] J. P. Cui, Y. L. Zhang, S. Zhang, and Y. Z. Wang. α -decay half-lives of superheavy nuclei. *Physical Review C*, 97:014316, 2018.
- [7] K. P. Santhosh, C. Nithya, H. Hassanabadi, and D. T. Akrawy. α -decay half-lives of superheavy nuclei from a modified generalized liquid-drop model. *Physical Review C*, 98:024625, 2018.
- [8] K. P. Santhosh and T. A. Jose. Alpha and cluster decay using modified generalized liquid drop model with iso-spin dependent pre-formation factor. *Nuclear Physics A*, 992:121626, 2019.
- [9] K. P. Santhosh, Dashty T. Akrawy, H. Hassanabadi, Ali H. Ahmed, and Tinu Ann Jose. α -decay half-lives of lead isotopes within a modified generalized liquid drop model. *Physical Review C*, 101:064610, 2020.
- [10] Y. J. Wang, H. F. Zhang, W. Zuo, and J. Q. Li. Improvement of a fission-like model for nuclear α decay. *Chinese Physics Letter*, 27:062103, 2010.
- [11] R. K. Gupta and W. Greiner. Cluster radioactivity. *International Journal of Modern Physics E*, 3:335–433, 1994.
- [12] B. B. Singh, S. K. Patra, and R. K. Gupta. Cluster radioactive decay within the preformed cluster model using relativistic mean-field theory densities. *Physical Review C*, 82:014607, 2010.
- [13] Jun-Gang Deng, Jie-Cheng Zhao, Peng-Cheng Chu, and Xiao-Hua Li. Systematic study of α decay of nuclei around the $Z = 82, N = 126$ shell closures within the cluster-formation model and proximity potential 1977 formalism. *Physical Review C*, 97:044322, 2018.
- [14] S. M. S. Ahmed, R. Yahaya, S. Radiman, and M. S. Yasir. *Journal of Physics G: Nuclear and Particle Physics*, 40:065105, 2013.
- [15] D. Deng and Z. Ren. α preformation factors of medium-mass nuclei and the structural effects in the region of crossing the $Z= 82$ shell. *Physical Review C*, 93:044326, 2016.
- [16] S. M. S. Ahmed. Alpha-cluster preformation factor within cluster-formation model for odd-A and odd-odd heavy nuclei. *Nuclear Physics A*, 962:103–121, 2017.
- [17] W. A. Yahya. Alpha decay half-lives of $^{171-189}\text{Hg}$ isotopes using modified gamow-like model and temperature dependent proximity potential. *Journal of the Nigerian Society of Physical Sciences*, 2:250–256, 2020.

- [18] A. Zdeb, M. Warda, and K. Pomorski. Half-lives for α and cluster radioactivity within a gamow-like model. *Physical Review C*, 87(2):024308, 2013.
- [19] G. Royer. Alpha emission and spontaneous fission through quasi-molecular shapes. *Journal of Physics G: Nuclear and Particle Physics*, 26(1149-1170):1149–1170, 2000.
- [20] G. Royer. Analytic expressions for alpha-decay half-lives and potential barriers. *Nuclear Physics A*, 848:279–291, 2010.
- [21] G. Royer, C. Schreiber, and H. Saulnier. Analytic relations for partial alpha decay half-lives and barrier heights and positions. *International Journal of Modern Physics E*, 20(4):1030–1033, 2011.
- [22] V. Viola and G. Seaborg. Nuclear systematics of the heavy elements - II Lifetimes for alpha, beta and spontaneous fission decay. *Journal of Inorganic and Nuclear Chemistry*, 28(3):741–761, 1966.
- [23] C. Qi, F. R. Xu, R. J. Liotta, R. Wyss, M. Y. Zhang, C. Asawatangtrakuldee, and D. Hu. Microscopic mechanism of charged-particle radioactivity and generalization of the geiger-nuttall law. *Physical Review C*, 80:044326, 2009.
- [24] C. Qi, F. R. Xu, R. J. Liotta, and R. Wyss. Universal decay law in charged-particle emission and exotic cluster radioactivity. *Physical Review Letters*, 103:072501, 2009.
- [25] Dashty T. Akrawy and Ali H. Ahmed. New empirical formula for α -decay calculations. *International Journal of Modern Physics E*, 27(8):1850068, 2018.
- [26] Z. Ren, C. Xu, and Z. Wang. New perspective on complex cluster radioactivity of heavy nuclei. *Physical Review C*, 70:034304, 2004.
- [27] D. T. Akrawy, H. Hassanabadi, Y. Qian, and K. P. Santhosh. Influence of nuclear isospin and angular momentum on α -decay half-lives. *Nuclear Physics A*, 983:310–320, 2019.
- [28] Mihai Horoi. Scaling behaviour in cluster decay. *Journal of Physics G: Nuclear and Particle Physics*, 30:945–955, 2004.
- [29] D. T. Akrawy and D. N. Poenaru. Alpha decay calculations with a new formula. *Journal of Physics G: Nuclear and Particle Physics*, 44:105105, 2017.
- [30] D. Naderi. *International Journal of Modern Physics E*, 22:1350065, 2013.
- [31] A. Adel and T. Alharbi. *Nuclear Physics A*, 958:187, 2017.
- [32] K. P. Santhosh, S. Sahadevan, B. Priyanka, and M. S. Unnikrishnan. *Nuclear Physics A*, 882:49, 2012.
- [33] T. T. Ibrahim, S. M. Wyngaardt, and B. D. C. KimeneKaya. *Nuclear Physics A*, 966:73, 2017.
- [34] A. Soylu, Y. Sert, O. Bayrak, and I. Boztosun. *European Physical Journal A*, 48:128, 2012.
- [35] A. Soylu, L. M. Robledo, and M. Warda. *International Journal of Modern Physics E*, 27:1850005, 2018.
- [36] D. Ni and Z. Ren. α -decay calculations of medium mass nuclei within generalized density-dependent cluster model. *Nuclear Physics A*, 828:348–359, 2009.

- [37] C. Xu and Z. Ren. *Nuclear Physics A*, 760:303–316, 2005.
- [38] C. Xu and Z. Ren. *Physical Review C*, 74:014304, 2006.
- [39] N. Maroufi, V. Dehghani, and S. A. Alavi. Cluster decay half-life with double-folding potential: Uncertainty analysis. *Acta Physica Polonica B*, 50(7):1349, 2019.
- [40] B. D. C. Kimene Kaya, S. M. Wyngaardt, T. T. Ibrahim, and W. A. Yahya. Comparison of double-folding effective interactions within the cluster model. *Physical Review C*, 2018.
- [41] F. Ghorbani, S.A. Alavi, and V. Dehghani. Temperature dependence of the alpha decay half-lives of even-even Th isotopes. *Nuclear Physics A*, 1002:121947, 2020.
- [42] Daming Deng and Zhongzhou Ren. Improved double-folding α -nucleus potential by including nuclear medium effects. *Physical Review C*, 96:064306, 2017.
- [43] I. I. Gontchar and M. V. Chushnyakova. A c-code for the double folding interaction potential of two spherical nuclei. *Computer Physics Communications*, 181:168–182, 2010.
- [44] G. R. Satchler D. T. Khoa and W. von Oertzen. *Physical Review C*, 54:954, 1997.
- [45] G. L. Zhang, H. Liu, and X. Y. Le. Nucleon-nucleon interactions in the double folding model for fusion reactions. *Chinese Physics B*, 18(1):136–141, 2009.
- [46] N. Maroufi, V. Dehghani, and S.A. Alavi. Alpha and cluster decay of some deformed heavy and superheavy nuclei. *Nuclear Physics A*, 983:77–89, 2019.
- [47] Meng Wang, W.J. Huang, F.G. Kondev, G. Audi, and S. Naimi. The AME 2020 atomic mass evaluation (ii). tables, graphs and references. *Chinese Physics C*, 45(3):030003, 2021.
- [48] W.J. Huang, Meng Wang, F.G. Kondev, G. Audi, and S. Naimi. The AME 2020 atomic mass evaluation (i). evaluation of input data, and adjustment procedures. *Chinese Physics C*, 45(3):030002, 2021.
- [49] F.G. Kondev, M. Wang, W.J. Huang, S. Naimi, and G. Audi. The NUBASE2020 evaluation of nuclear physics properties. *Chinese Physics C*, 45(3):030001, 2021.